Feature Extraction Method for Epileptic Seizure Detection Based on Cluster Coefficient Distribution of Complex Network

[1,2] FENGLIN WANG, [1,2,*] QINGFANG MENG, [1,2] YUEHUI CHEN, [3] YUZHEN ZHAO
[1] School of Information Science and Engineering
University of Jinan
Jinan, Shandong
CHINA
[2] Shandong Provincial Key Laboratory of Network Based Intelligent Computing
Jinan, Shandong
CHINA
[3] School of Management Science and Engineering
Shandong Normal University
Jinan, Shandong
CHINA
[*]ise_mengqf@ujn.edu.cn

Abstract: - Automatic epileptic seizure detection has important research significance in clinical medicine. Feature extraction method for epileptic EEG occupies core position in detection algorithm, since it seriously affects the performance of algorithm. In this paper, we propose a novel epileptic EEG feature extraction method based on the statistical property of complex networks theory. EEG signal is first converted to complex network and cluster coefficients of every node in the network are computed. Through analysis of the cluster coefficient distribution, the partial sum of cluster coefficient distribution is extracted as the classification feature. A public epileptic EEG dataset was utilized for evaluating the classification performance of extracted feature. Experimental results show that the extracted feature achieves classification accuracy up to 94.50%, which indicates that it can clearly distinguish between the ictal EEG and interictal EEG. The higher classification accuracy demonstrates the extracted classification feature's great potentiality of the real-time epileptic seizures detection.

Key-Words: - Epileptic Seizure Detection, Feature Extraction Method, Complex Network, Cluster Coefficient Distribution, Nonlinear Time Series Analysis, Electroencephalograph (EEG)

1 Introduction

Epilepsy is one of the most common neurological disorders and has significant impacts, such as temporary impairments of perception, speech, motor control, memory or consciousness, on patient daily life. Symptom of epilepsy attack is that a person has repeated seizures or convulsions. Nearly one out of three epilepsy patients cannot obtain treatment [1], because the epilepsy attacks are completely sudden and unforeseen. Moreover, traditional epileptic seizure detection, which needs time-consuming observation and analysis of the entire length of electroencephalograph (EEG) by a neurologist, is a tedious and subjective diagnostic process.

With the advent of technology, the digital EEG data can be fed into an automated seizure detection system implemented by computer. Epileptic seizure detection problem is then modelled as EEG signals classification problem by computer. Analysis time is reduced considerably due to automation and the neurologist can treat more patients in a given time. Base on several classification algorithms, automatic epileptic seizure detection has been implemented but still has significant importance in clinic. The techniques for epileptic EEG classification contain two primary parts, which are the feature extracted method and classifier design. The feature extraction method extracts several objective quantitative features, which can clearly characterize the fundamental difference between the research objects and is then used as the representative of the research object. Brain activity during an epileptic seizure stage differs greatly from that in the normal state. An ideal classification feature contains only intrinsic

information of the object, which means that the extracted feature can catch the different characteristics between various objects and get much better classification performance. According to growing awareness that the electrical activities of the brain are complex nonlinear dynamic systems [1], compared to the linear features, nonlinear features are more suitable for characterizing the nature of EEG.

Numerous nonlinear features of EEG signals have been applied into the analysis of EEG signals, recently [2-12]. Based on largest Lyapunov exponent, reference [2] discussed the detection and prediction of epileptic seizure. Reference [3] analyzed the correlation dimensions of epileptic EEGs, and concluded that the correlation dimension of the epileptic EEG is larger than the normal EEG's. Higher order spectral analysis (HOS) is a powerful tool for the nonlinear dynamical analysis of nonlinear, non-stationary and non-Gaussian physiological signals. In [4,5], HOS were used to analyze epileptic EEG signals and extracted useful features which could be used to detect epileptic seizures. In [6,7], the third order cumulant (3rd HOC) which highlights the nonlinear behaviour was used for analyzing epileptic EEG signals. The Hurst exponent of the epileptic EEG was discussed in [8] and the results shown that the normal EEG is uncorrelated whereas the epileptic EEG is long range anti-correlated. Spectral entropy and embedding entropy, which can be used to measure the system complexities, were introduced to epilepsy detection in [9,10]. The recurrence quantification analysis (RQA), which is used to analysis the recurrence plot (RP), gives parameters that measure the complexity and nonlinearity of the non-stationary data. Acharya *et al*. [11] used RQA features for the three-class classification of epilepsy EEG signals. Combined with these classification features, the classifiers, such as artificial neural network (ANN) and support vector machine (SVM), have also been widely applied into the epilepsy detection algorithm [12-17]. From these literatures, we can conclude that an excellent classification feature not only obtains better classification accuracy but also spends less computational complexity because of it does not need combined with classifier. These advantages are significant for the clinical application.

Recently, complex networks theory shows its advantages in analysis of nonlinear time series. Zhang and Small [18] proposed the pioneering algorithm that converted the pseudo-periodic time series into complex network. A bridge between nonlinear time series analysis and complex networks theory has been built. After that, various conversion algorithms were proposed and the complex network method has been applied into several application fields. Reference [19] converted time series into complex network based on time delay embedding theory, and shown, compared with pseudo-periodic time series, that the chaos attractor reveals a more heterogeneous structure and exhibits small world feature. In [20] and [21], the transition network, another type of complex network, was applied into the analysis of the traffic flow time series and random process, respectively. Yang *et al*. [22] constructed the correlation complex network of time series under different dynamics, which was based on the time delay embedding theory and the similarity between the two nodes was measured by correlation coefficient. Lacasa *et al*. [23] first proposed the visibility graph algorithm, which could convert arbitrary time series into a network. Marwan *et al*. [24] constructed the recurrence network of time series and made some comparison with the RQA. He proved that the topology statistical properties of complex network could capture transfer dynamics characteristic of time series. Gao and Jin [25] used the directed weighted complex network, which can reserve more information about the series, to analyze the time series. Based on these conversion algorithms, the nonlinear time series dynamics were analyzed. In [26], the super-family phenomena that the set of complex networks with the same relative abundance of the different sub-graph was discovered and defined. Liu *et al*. [27] unveiled that the detrended fluctuation analysis (DFA) scaling exponent of the time series uniquely determines the classification of the super-family phenomenon. Tang *et al*. [28] applied the complex networks theory into the analysis of the topology characteristics of the non-stationary traffic-flow time series network. Through the conversion algorithm, time series is mapped into the phase space, and we can analyze its dynamic structures by plenty of statistical properties of complex networks theory. Complex networks theory provides a new perspective for dynamics analysis of nonlinear time series

In this paper, a new classification feature extracted method for epileptic seizure detection is proposed. Firstly, the EEG signal is converted into the complex network. Then the cluster coefficients of every nodes and the cluster coefficient distribution of the resulting complex network are calculated. At last, partial sum of cluster coefficient distribution, which is extracted as the classification feature, is utilized to describe the differences between the epileptic EEGs at different stages. A

classification experiment, which utilizes the extracted feature for distinguishing the ictal EEGs from the interictal EEGs, is used to verify the classification performance of the extracted feature.

This paper has been organized as follows. Section 2 presents the algorithm for converting the time series into weighted network, and focuses on describing the feature extraction method for automatic epileptic seizure detection. In Section 3, the EEG signal benchmark dataset and the evaluation parameters used in the classification experiment are described. Then the experimental results are presented. Finally, some conclusions are included in Section 4.

2 Methods

The main idea of applying the complex network theory into the analysis of the dynamics of the nonlinear time series is: (1) map the time series into the complex network domain and (2) use the topology structure statistical properties provided by the complex network theory to analyze the time series complex network (TSCN).

2.1 Algorithm for Converting the Time Series into Complex Network

A time series is denoted as

$$\{s_1, s_2, ..., s_j, ..., s_m\} \left(j \in [1, m]\right), \quad (1)$$

where the s_j is the j_{th} sample point in time series and the length of the series is m.

A complex network composes of node set and edge set.

In order to construct the node set of the TSCN, the nonlinear time series is divided up into several individual cycles and each cycle is then treated as a node in the TSCN. According to the local minimum (or maximum) values, the time series is divided up into several non-overlapping cycles and the cycle set is denoted as $\{c_1, c_2, ..., c_N\}$, where c_j represents the j_{th} cycle divided from the time series. Obviously, the number of cycles in the cycle set, N, is related to the amount of local minimum (or maximum) values. Points before the first local minimum (or maximum) values and after the last local minimum (or maximum) values are abandoned. Each cycle is then treated as a node in the TSCN and the node set is obtained.

The complex network edge set contains a number of edges, which represent the connections between nodes in the TSCN. The similarity between the two nodes is used as a standard to judge whether the two nodes connect each other or not. From the view of high-dimensional phase space, the distance between two nodes c_i and c_j is described by Euclidean distance, denoted as d_{ij}. Since the cycles have different length, the Euclidean distance is modified as

$$d_{ij} = \min_{l=0,1,..,L_j-L_i} \left(\frac{1}{L_i} \sqrt{\sum_{k=1}^{k=L_i} \left(c_i(k) - c_j(k+l)\right)^2} \right), \quad (2)$$

where $c_i(k)$ is the k_{th} point in c_i. The lengths of c_i and c_j are L_i and L_j, respectively (assuming $L_i<L_j$). Two nodes with a smaller distance are closer in phase space, which means that the two nodes are more similar. After a pair wise high-dimensional distance computing between every two nodes in TSCN, a distance similarity matrix is obtained, denoted as $D = \left(d_{ij}\right)_{N \times N}$.

The edge between two nodes is determined by equation (3).

$$a_{ij} = \begin{cases} 1 & d_{ij} < \varepsilon \\ 0 & d_{ij} \geq \varepsilon \end{cases}, \quad (3)$$

where the ε is a predetermined value used to construct an edge between the two nodes which have bigger similarity. The a_{ij} = 1 means that there is an edge between the i_{th} node and the j_{th} node, whereas a_{ij} = 0 means there is no edge between two nodes.

With an appropriate critical value ε selected, the distance similarity matrix D is converted into a binary matrix $A = \left(a_{ij}\right)_{N \times N}$, namely adjacency matrix. Since the adjacency matrix A contains the node set and edge set of the network, it can fully represent the entire TSCN.

In the conversion algorithm, the parameters ε, which may seriously affect the performance of the TSCN, need to be settled. It determines whether the embedded dynamics of time series can be sufficient encoded into the topological structure of the TSCN or not. When ε is extremely large, the nodes with weak similarities are also connected, which result in that the physically meaningful correlations of time series are submerged by the noises. With ε decreased, more and more noises can be filtered out. The ε cannot be extremely small, since some connections with physical significance may be filtered out. Moreover, due to a small finite number of connections caused by the extremely small ε, strong statistical fluctuations may appear. The widely used determination of the threshold ε is based on the changes of network density [19], which is suitable for the complex networks with hierarchical structure. In order to investigate the

neighbours' structure of every node in the TSCN, the total number of edges in the TSCN is fixed as 5% of the total number of all possible edges [26], which is realized as follow:

1) Ranking all the elements of the distance similarity matrix D (except elements of principal diagonal) in ascending order;

2) Finding out the $(2\times0.05\times N\times(N-1)+1)_{th}$ element. This element is the value of the ε.

2.2. Analysis of the Time Series Complex Network Based on Complex Network Theory

Since the adjacency matrix A contains the detailed information of the entire TSCN, the analysis of TSCN can be realized by studying the matrix A.

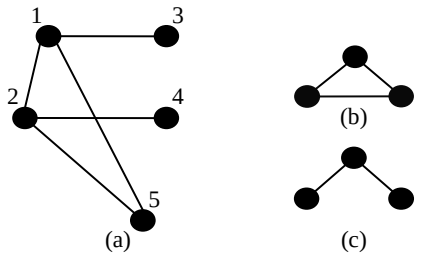

Fig.1 A sample complex network with 5 nodes and 5 edges (a). (b) The complete triangle and (c) the triangular graph.

In TSCN, every node interrelates to its neighbours (except isolated node). Two neighbours of a node may be neighbours themselves. The clustering coefficient is a feature which characterizes the presence of order three loops. The clustering coefficient of the i_{th} node is defined as

$$C_i = \frac{N_\Delta(i)}{N_3(i)}, \tag{4}$$

where $N_\Delta(i)$ is the number of complete triangles with the i_{th} node and $N_3(i)$ is the number of connected triples with the i_{th} node, respectively shown in Fig.1 (b) and (c). A triangle is a set of three vertices with edges between each pair of vertices; a connected triple is a set of three vertices where each vertex can be reached directly or indirectly from each other, i.e., two vertices must be adjacent to another vertex which is called as the central vertex. It can be seen from Fig.1 that each triangle can be seen as consisting of three different connected triples, one with each of the vertices as central vertex.

In TSCN, the $N_\Delta(i)$ and the $N_3(i)$ can be calculated through equation (5) and (6), respectively.

$$N_\Delta(i) = \sum_{k>j} a_{ij}\cdot a_{ik}\cdot a_{jk}, \tag{5}$$

$$N_3(i) = \sum_{k>j} (a_{ij}\cdot a_{ik} + a_{ji}\cdot a_{jk} + a_{ki}\cdot a_{kj}), \tag{6}$$

where the a_{ij} is the element of the adjacency matrix A and the sum is taken over all triples of distinct vertices j and k only one time. Considered the example shown in the Fig.1, since node 1 has 1 complete triangle and 3 triangular graphs (i.e., 3-1-2, 5-1-2, 3-1-5), so the C_1=1/3.

Obviously, $0\le C\le 1$, C=0 if and only if all neighbours are unconnected for any node in the network and C=1 if and only if all nodes are connected each other, such as a set of isolated nodes and a fully connected regular network, respectively. Its has been a common observation that cluster coefficients of the most real-world networks satisfy $O(N^{-1})<<C<<1$, which indicates that most real-world networks are neither completely random nor completely regular.

2.3 Feature Extraction Method Based on the Cluster Coefficient Distribution

Cluster coefficient characterizes the proportion of that the neighbour nodes between each other are also neighbours, i.e., the perfect degree of small group structure. The C_i characterizes the regularity degree of neighbours of the i_{th} node.

According the awareness that the dynamic structure of interictal EEG signal shows more complex than the ictal EEG dynamic structure [1], which means that the dynamic structure of interictal EEG is more irregular than the dynamic structure of ictal EEG, we defines clustering coefficient distribution (CCD) of TSCN and uses it to analyze the irregular degree of TSCN:

$$P(I) = \frac{\sum_{i=1}^{N} true(C_i \in s_I)}{N}, \tag{7}$$

where the I in (7) is an integer in the interval [1 12]. The symbol '*ture*()' is used for judging the true or false of the expression in the parenthesis. When the expression in the parenthesis is true, the symbol '*ture*()' is 1, otherwise is 0.

In order to facilitate subsequent analysis, the cluster coefficients belong to the interval [0 1] are divided up into 12 subintervals, as equation (8),

$$S = \begin{Bmatrix} s_1 = \{0\}; & s_{12} = \{1\}; & s_{11} \in (0.9 \quad 1); \\ s_i \in (0.1\cdot(i-2) & 0.1\cdot(i-1)] \,|\, i \in [2 & 10] \end{Bmatrix}. \tag{8}$$

Since smaller C_i means imperfect small group, which indicates irregularity, the sum of $P(I)$s from the 2_{nd} to the 6_{th} subintervals, corresponding to the interval (0 0.5], is extracted as the feature, defined as

$$P_{clu} = \sum_{I=2}^{6} P(I). \quad (9)$$

Time series with different dynamics have various TSCN structures, i.e. the shapes of their CCDs are different. When the extracted feature P_{clu} is larger, the TSCN may have many nodes with smaller cluster coefficient, which means that the TSCN is more irregular.

3 Results and Discussion

3.1 Data Description

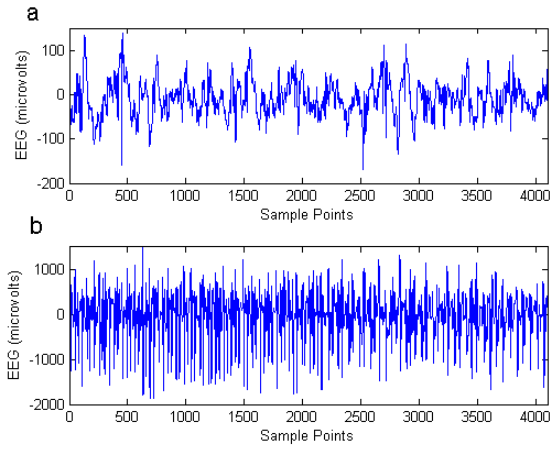

Fig.2 The typical EEG waveforms corresponding to epilepsy: a) an interictal EEG sample in dataset D, b) an ictal EEG sample in dataset E. The length of each EEG sample is 4097.

In this paper, the public database [29], came from Department of Epileptology, Bonn University, Germany, is used for testing classification performance of the extracted feature. The EEG dataset D and dataset E are used in the classification experiment, each of which contained 100 single-channel EEG data of 23.6 s time duration. The dataset D was composed of intracranial EEGs recorded during interictal periods. The EEG signals in dataset E were recorded during ictal periods. They were all measured through using deep electrodes placed within the epileptogenic zone of the brain. The EEGs of two datasets were taken from five epileptic patients experiencing pre-surgical diagnosis. All EEG signals were recorded with the same 128-channel amplifier and digitized at 173.6 samples per second at 12-bit resolution. Each datum had 4097 sampling points. Fig.2 (a) and (b) depict examples of interictal EEG and ictal EEG, respectively.

3.2 Performance Evaluation Parameters

In experiment section, the interictal EEGs and the ictal EEGs are regarded as the positive class and the negative class, respectively. The classification performance of the extracted feature is evaluated by using parameters such as sensitivity (*SEN*), specificity (*SPE*), and overall accuracy (*ACC*), which are shown in equations (10), (11), and (12), respectively[14].

$$SEN = \frac{TP}{TP + FN}, \quad (10)$$

the number of true positives (*TP*) divided by the total number of interictal EEG signals labelled by the EEG experts. *TP* stands for the interictal EEG signals recognized by both the detection algorithm and the EEG experts. False negative (*FN*) is the number of interictal signals labelled epileptic by the detection algorithm.

$$SPE = \frac{TN}{TN + FP}, \quad (11)$$

the number of true negatives (*TN*) divided by the total number of ictal EEG signals labelled by the EEG experts. *TN* stands for the ictal EEG signals recognized by both the detection algorithm and the EEG experts. False positive (*FP*) is the number of epileptic signals labelled interictal by the detection algorithm.

$$ACC = \frac{TP + TN}{TP + FN + TN + FP}, \quad (12)$$

the number of correctly recognized EEG signals (*TP*+*TN*) divided by the total number of EEG signals.

3.3 Classification Experiment Results and Discussion

In this experiment section, the local maximum values of the EEG signals are used for time series segmentation. For the purpose of testing the classification performance of the extracted feature, two hundred interictal EEG samples and 200 ictal EEG samples, which are respectively taken out from the dataset D and dataset E, constitute the test set. Each original datum in the two datasets is divided up into two equal-length sections of 2048 points and

the two sections are used as two independent samples. Then the time series complex networks (TSCN) of the 400 test samples are constructed and the cluster coefficient distributions (CCD) of all the resulting TSCNs are calculated.

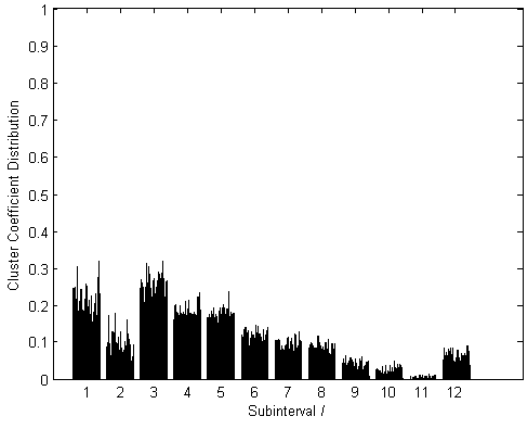

Fig.3 The cluster coefficient distributions of the resulting complex networks constructed from the 200 interictal test EEG samples in the test dataset. The length of each test sample is 2048.

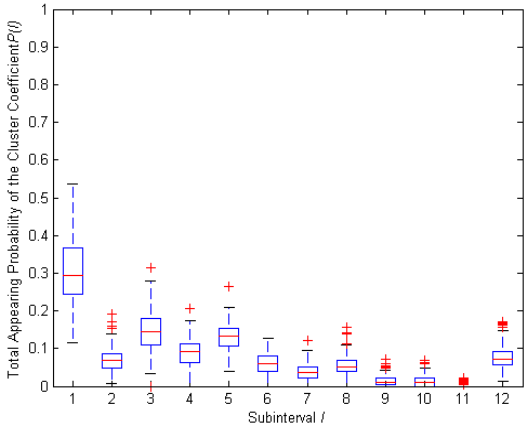

Fig.4 The boxplots for total appearing probabilities of the cluster coefficients belong to the I_{th} subinterval shown in Fig.3.

According to equation (7), $P(I)$ is total appearing probability of cluster coefficients belong to the I_{th} subinterval. The CCD of one EEG test sample contains twelve $P(I)$s. In order to find the similarity of CCDs in each category and the difference of CCDs between two categories, in Fig.3 the I_{th} total appearing probabilities $P(I)$s, which come from every interictal test samples' CCD, are shown together in the I_{th} subinterval, and all the same to the CCDs of ictal test samples, shown in Fig.5.

In Fig.4 and Fig.6, the I_{th} boxplot contains 200 $P(I)$s in the I_{th} subinterval come from the interictal test EEGs or the ictal test EEGs, respectively. These boxplots may clearly display the distribution of $P(I)$s, i.e., two hundred total appearing probabilities of cluster coefficient in the I_{th} subinterval.

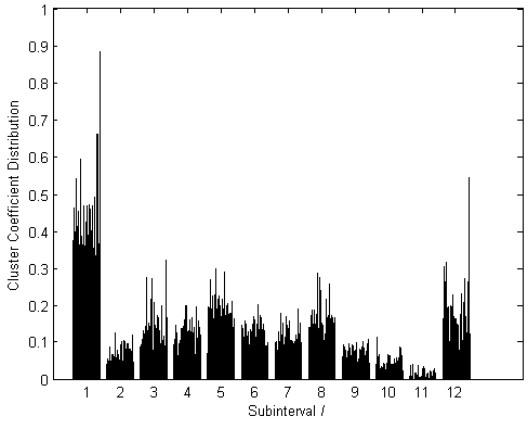

Fig.5 The cluster coefficient distributions of the resulting complex networks constructed from the 200 ictal test EEG samples in the test dataset. The length of each test sample is 2048.

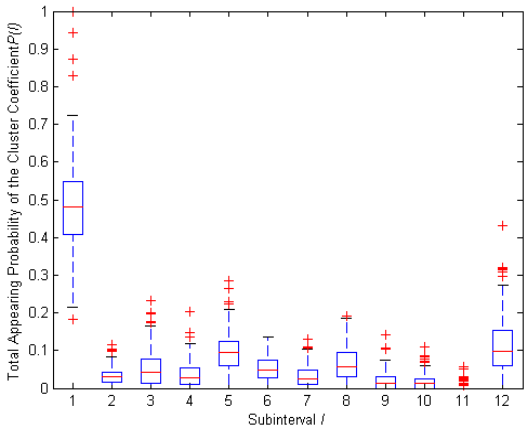

Fig.6 The boxplots for total appearing probabilities of the cluster coefficients belong to the I_{th} subinterval shown in Fig.5.

It can be seen from Fig.3 that, for all the interictal test samples, $P(I)$s in each subinterval I are very similar. For the ictal test EEG samples shown in Fig.5, the same conclusion is obtained. That is to say that the CCDs of the samples in the same category, such as ictal set or interictal set, have very similar distribution form.

In Fig.4, $P(3)$ in the 3_{rd} subinterval distributes near 0.1943, whereas $P(3)$ distributes near 0.0642 in Fig.6. The $P(4)$ and $P(6)$ distribute near 0.1470 and 0.0930 in Fig.4, respectively, whereas the $P(4)$ and $P(6)$ distribute near 0.0617 and 0.0824 in Fig.6, respectively. These results suggest that the CCD shapes of interictal test samples are significant different from the CCD shapes of ictal test samples.

Moreover, the TSCN of interictal EEG has more nodes with smaller cluster coefficients, whereas the TSCN of ictal EEG has more nodes with large cluster coefficients. It can be concluded that the TSCN of interictal EEG is more complex (irregular) than the TSCN of ictal EEG. This confirms the conclusion [1] that the time series dynamic under epileptic interictal period is more complex than epileptic ictal period.

The observed result and obtained conclusion indicate that the extracted feature P_{clu} can clearly characterize the difference between the dynamics of the EEG signals under different brain conditions in TSCN domain. Therefore the P_{clu} can be extracted as the classification feature to distinguish between the two kinds of EEG signals.

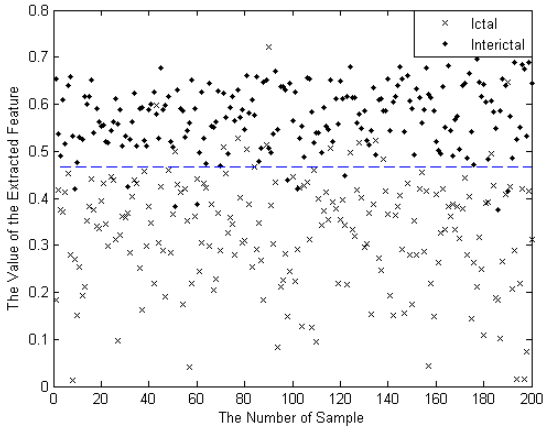

Fig.7 The classification result of the extracted feature by a straight line. The classification accuracy is 94.50%.

The distribution of 400 P_{clu}s is shown in Fig.7, where each 'x' represents P_{clu} of one ictal test sample and each '•' represents P_{clu} of one interictal test sample. It also can be found that the P_{clu}s of ictal test samples are smaller than the interictal test samples except several special samples. Only 9 interictal test samples and 13 ictal test samples are put into wrong category when the test samples are classified by the dotted line (0.4673) shown in Fig.7. The classification accuracy is 94.50% (with the sample length L is 2048). In Table 1, the classification performance of the approximate entropy and sample entropy, which are also utilized as extracted feature to classify the same test set (the sample length is 2048), are used to compare with the classification performance of the extracted feature. The average run times of these feature extraction methods are also listed in Table 1. A conclusion can be drawn from the Table 1 that the extracted feature P_{clu} shows the best performance not only in classification *SEN* and *SPE*, but also in *ACC*. The run time taken by feature extraction method (L=2048) is slightly longer than the run time taken by other two entropies and the time of feature extraction is only 17.33% of the sample duration (11.8785 s).

Table 1 The classification results of the proposed feature and two other features for comparison

Feature	*SEN* (%)	*SPE* (%)	*Run Time*(s)	*ACC* (%)
Approximate Entropy	83.00	91.50	1.96 ±0.36	87.25
Sample Entropy	91.50	84.00	1.86 ±0.34	87.75
$P_{clu(2048)}$	95.50	93.50	2.06 ±0.16	94.50
$P_{clu(1024)}$	91.50	91.50	0.66 ±0.01	91.50

Table 2 lists the accuracies of several established epilepsy automatic classification algorithms, which are combined with the SVM classifier and applied to the same epileptic EEG dataset. Here, the DFA-α is the scaling exponent of the detrended fluctuation analysis of epileptic EEG. The results of approximate entropy combined with SVM and sample entropy combined with SVM are obtained based on the results listed in Table 1. Table 2 shows that the single feature classification algorithm based on the P_{clu} proposed in this study achieves the highest classification accuracy compared with other established classification algorithms, which combined with classifier. To some extent, this result also shows that the feature, P_{clu}, extracts more essential information than other features listed in Table 2, which makes P_{clu} conform to the main purpose of the feature extraction method.

Table 2 The classification accuracies of different epileptic EEG classification algorithms applied into the same epileptic EEG dataset

Feature	*ACC* (%)
DFA-α + SVM[10]	82.00
Hurst + SVM[11]	87.25
Approximate Entropy + SVM	89.00
Sample Entropy + SVM	91.00
Single feature classification based on P_{clu}	94.50

In order to investigate whether the length of sample affects the classification performance of the

extracted feature, each datum in the two epileptic EEG datasets is divided into four equal-length sections of 1024 points. The 2_{nd} section and the 4_{th} section are regarded as two different test samples. In this way, two hundred ictal test samples and 200 interictal test samples constitute a new test set. The same analysis procedure is then applied to the new test set. From Fig.8 to Fig.11, the results of the CCDs and the corresponding boxplots for the two different kinds of EEG signals are displayed.

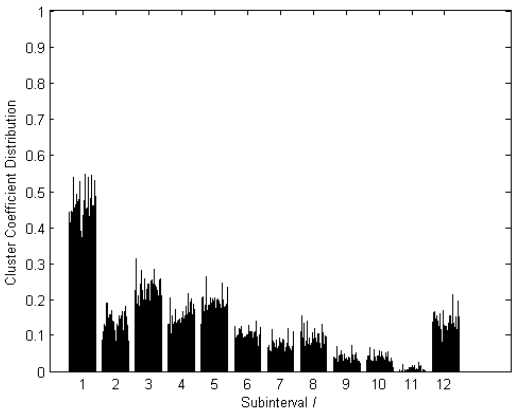

Fig.8 The cluster coefficient distributions of the resulting complex networks constructed from the 200 interictal test EEG samples in the second test dataset. The length of each test sample is 1024.

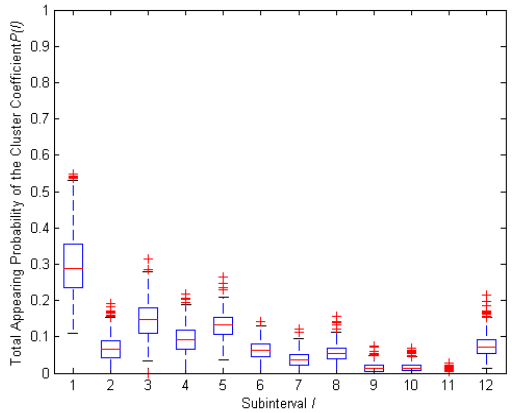

Fig.9 The boxplots for total appearing probabilities of the cluster coefficients belong to the I_{th} subinterval shown in Fig.8.

The classification result of the extracted feature under the short data length is shown in Fig.12. The classification performance evaluation parameters, *SEN*, *SPE*, and *ACC* are listed in Table 1 (*L* is 1024). Compared with sample length is 2048, the *ACC* of the extracted feature under short length is slightly lower, about 91.50%, but the feature extraction time is much shorter, only 0.66 s. It can be concluded that as the data length become short the classification accuracy of the extracted feature is slightly low, but the feature extraction time has decreased significantly.

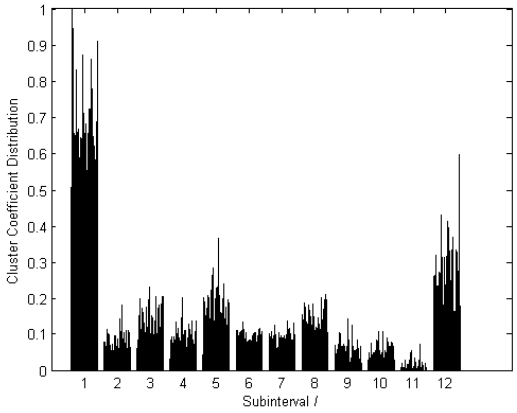

Fig.10 The cluster coefficient distributions of the resulting complex networks constructed from the 200 ictal test EEG samples in the second test dataset. The length of each test sample is 1024.

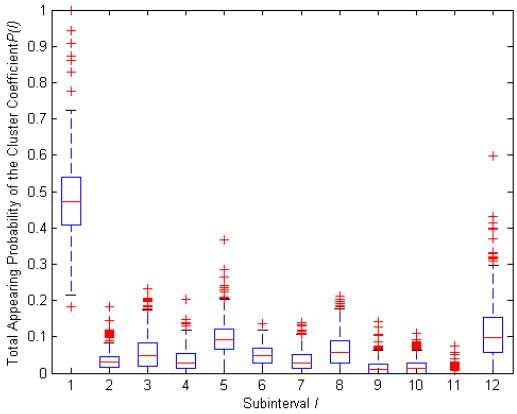

Fig.11 The boxplots for total appearing probabilities of the cluster coefficients belong to the I_{th} subinterval shown in Fig.10.

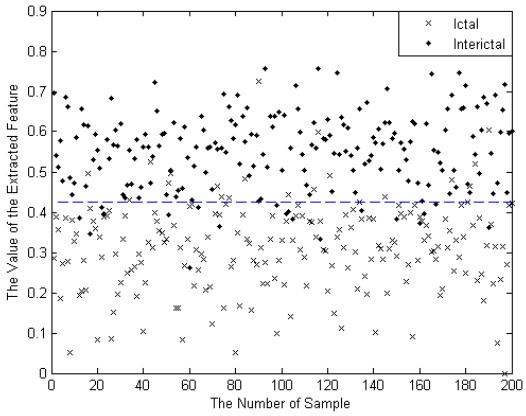

Fig.12 The classification result of the extracted feature by a straight line. The classification accuracy is 91.50%.

4 Conclusion

In this paper, a novel feature extraction method for epileptic EEG is proposed, which can be applied into the detection of interictal EEG and ictal EEG. The proposed scheme firstly construct the node set of time series complex network (TSCN) according to local maximum and the edge set of TSCN is constructed based on the similarity between every two nodes. Then the cluster coefficients of all the nodes in the TSCN and the cluster coefficient distribution (CCD) are calculated. At last, the partial sum of CCD, P_{clu}, is defined and extracted as the classification feature. The classification performance of P_{clu} is evaluated by classifying two kinds of epileptic EEGs. Experimental results show that the P_{clu} can clearly describe the essential difference between the two kind signals and achieves the higher classification accuracy up to 94.50% (L=2048). The feature extraction time for one EEG sample with 2048 sampling points is approximately 2.06 s, which is shorter than the EEG sample's time duration (11.8 s). Taking into account these advantages, the feature proposed in this paper shows its great potentiality for real-time detection of epileptic seizure.

Acknowledgment

This work was supported by the National Natural Science Foundation of China (Grant No. 61201428, 61070130), the Natural Science Foundation of Shandong Province, China (Grant No. ZR2010FQ020), the China Postdoctoral Science Foundation (Grant No. 20100470081), the Program for Scientific Research Innovation Team in Colleges and Universities of Shandong Province.

References

[1] U. Rajendra Acharya, S. Vinitha Sree, G. Swapna, Roshan Joy Martis, Jasjit S. Suri, Automated EEG analysis of epilepsy: A review, *Knowledge-Based Systems*, Elsevier, Vol.45, 2013, pp. 147–165.

[2] S. Osowski, B. Swiderski, A. Cichocki and A.Rysz, Epileptic seizure characterization by Lyapunov exponent of EEG signal, *COMPEL: The International Journal for Computation and Mathematics in Electrical and Electronic Engineering*, Emerald, Vol.26, No.5, 2007, pp. 1276–1287.

[3] H. Jing, M. Takigawa, Topographic analysis of dimension estimates of EEG and filtered rhythms in epileptic patients with complex partial seizures, *Biol. Cybern.*, Springer, Vol.83, No.5, 2000, pp. 391–397.

[4] U.R. Acharya, S. Vinitha Sree, J.S. Suri, Automatic detection of epileptic EEG signals using higher order cumulant features, *Int. J. Neural Syst*., World Scientific, Vol.21, No.5, 2011, pp. 403–414.

[5] K.C. Chua, V. Chandran, U.R. Acharya, C.M. Lim, Application of higher order spectra to identify epileptic EEG, *J. Med. Syst.*, Springer, Vol.35, No.6, 2011, pp. 1563–1571.

[6] D. Yao, Electroencephalography inverse problem by subspace decomposition of the fourth-order cumulant matrix, *J. Biomed. Eng.*, Europe PMC, Vol.17, No.2, 2000, pp. 174–178.

[7] A.E. Villa, I.V. Tetko, Cross-frequency coupling in mesiotemporal EEG recordings of epileptic patients, *J. Physiol.*, Elsevier, Vol.104, No.3, 2010, pp. 197–202.

[8] M. Nurujjaman, N. Ramesh, A. N. Sekar Iyengar, Comparative study of nonlinear properties of EEG signals of normal persons and epileptic patients, *Nonlin. Biomed. Phys.*, Springer, Vol.3, No.1, 2009, pp. 6.

[9] U.R. Acharya, F. Molinari, S. Vinitha Sree, S. Chattopadhyay, Ng. Kwan-Hoong, J.S. Suri, Automated diagnosis of epileptic EEG using entropies, *Biomed. Signal Process Control*, Elsevier, Vol.7, No.4, 2012, pp. 401–408.

[10] N. Kannathal, C.M. Lim, U.R. Acharya, P.K. Sadasivan, Entropies for detection of epilepsy in EEG, *Comput. Methods Programs Biomed.*, Elsevier, Vol.80, No.3, 2005, pp. 187–194.

[11] U.R. Acharya, S. Vinitha Sree, S. Chattopadhyay, Y.U. Wenwei, A.P.C. Alvin, Application of recurrence quantification analysis for the automated identification of epileptic EEG signals, *Int. J. Neural Syst.*, World Scientific, Vol. 21, No.3, 2011, pp. 199–211.

[12] E. D. übeyli, Combined neural network model employing wavelet coefficients for EEG signals classification, *Digital Signal Processing*, Elsevier, Vol.19, No.2, 2009, pp. 297–308.

[13] Tapan Gandhi, Bijay Ketan Panigrahi, Manvir Bhatia, Sneh Anand, Expert model for detection of epileptic activity in EEG signature, *Expert Systems with Applications*, Elsevier, Vol.37, No.4, 2010, pp. 3513–3520.

[14] Y. Song, P. Liò, A new approach for epileptic seizure detection sample entropy based feature extraction and extreme learning machine, *Journal of Biomedical Science and Engineering*, Vol.3, No.6, 2010, pp. 556–567.

[15] Qi Yuan, Weidong Zhou, Yinxia Liu, Jiwen Wang, Epileptic seizure detection with linear and nonlinear features, *Epilepsy & Behavior*, Elsevier, Vol.24, No.4, 2012, pp. 415–421.

[16] Qi Yuan, Weidong Zhou, Shufang Li, Dongmei Cai, Epileptic EEG classification based on extreme learning machine and nonlinear features, *Epilepsy Research*, Elsevier, Vol.96, No.1, 2011, pp. 29–38.

[17] Cai Dong-Mei, Zhou Wei-Dong, Liu Kai, Li Shu-Fang, Geng Shu-Juan, Approach of epileptic EEG detection based on Hurst exponent and SVM, *Chinese Journal of Biomedical Engineering*, Vol.29, No.6, 2010, pp. 836–840.

[18] J. Zhang, M. Small, Complex network from pseudoperiodic time series: Topology versus dynamics, *Physical Review Letters*, APS, Vol.96, No.23, 2006, 238701.

[19] J. Wu, H. Sun and Z. Gao, Mapping to complex networks from chaos time series in the car following model, *Traffic and Transportation Studies*, ASCE, 2008, pp. 397–407.

[20] Z. Y. Gao, K. P. Li, Evolution of traffic flow with scale-free topology, *Chinese Phys. Lett.*, IOP, Vol.22, No.10, 2005, pp. 2711–2714.

[21] G. Nicolis, A. G. Cantu´, C. Nicolis, Dynamical aspects of interaction networks, *International Journal of Bifurcation and Chaos*, World Scientific, Vol.15, No.11, 2005, pp. 3467–3480.

[22] Yue Yang, Huijie Yang, Complex network-based time series analysis, *Physica A*, Elsevier, Vol.387, No.5, 2008, pp. 1381–1386.

[23] L. Lacasa, B. Luque, F. Ballesteros, J. Luque, JC. Nuno, From time series to complex networks: The visibility graph, *Proc.Natl. Acad. Sci.* National Acad Sciences USA, Vol.105, No.13, 2008, pp. 4972–4975.

[24] N. Marwan, J. F. Donges, Y. Zou, R. V. Donner, J. Kurths, Complex Network Approach for recurrence analysis of time series, *Physics Letters A*, Elsevier, Vol.373, No.46, 2009, pp. 4264–4254.

[25] Z. K. Gao, N. D. Jin, A directed weighted complex network for characterizing chaotic dynamics from time series, *Nonlinear Analysis: Real World Applications*, Elsevier, Vol.13, No.2, 2012, pp. 947–952.

[26] X. Xu, J. Zhang, M. Small, Superfamily phenomena and motifs of networks induced from time series, *Proc. Natl. Acad. Sci.* National Acad Sciences USA, Vol.105, No.50, 2008, pp. 19601–19605.

[27] C. Liu, W. X. Zhou, Superfamily classification of nonstationary time series based on DFA scaling exponents, IOP, *J. Phys. A: Math. Theor.*, Vol.43, No.49, 2010, 495005.

[28] Jinjun Tang, Yinhai Wang, Fang Liu, Characterizing traffic time series based on complex network theory, *Physica A: Statistical Mechanics and its Applications*, Elsevier, Vol.392, No.18, 2013, pp. 4192–4201.

[29] Ralph G. Andrzejak, Klaus Lehnertz, Florian Mormann, Christoph Rieke, Peter David, and Christian E. Elger, Indications of nonlinear deterministic and finite-dimensional structures in time series of brain electrical activity: Dependence on recording region and brain state, *Physical Review*, APS, Vol.64, No.6, 2001, 061907.